

Current Developments in Airborne SAR Remote Sensing

**OLAF HELLWICH, ANDREAS REIGBER, STEPHANE GUILLASO, MARC JÄGER,
MAXIM NEUMANN, ANKE BELLMANN, Berlin**

ABSTRACT

In the recent past, airborne Synthetic Aperture Radar (SAR) remote sensing has witnessed several principal and technical improvements. In particular, spatial resolution has been increased significantly, polarimetric SAR, polarimetric interferometric SAR, and tomographic SAR were introduced, and repeat-pass interferometric SAR was developed for airborne SAR sensors. These advances have made possible numerous new applications, including urban structure and object detection and characterization.

In this paper we describe current challenges in the continued development of airborne SAR systems. We illustrate the description by research work conducted at Berlin University of Technology in the time period from 2002 to 2005.

1. INTRODUCTION

Airborne SAR remote sensing requires optimal data processing on several levels to achieve the best possible spatial and radiometric resolution, as well as interferometric phase accuracy. As the processing chain between the acquisition of raw data by the SAR sensor, and the input of extracted and characterized objects into a geoinformation system is often subdivided between several institutional units, is desirable to be able to flexibly adjust data processing steps to suit a particular input/output scenario, and maintain optimality with respect to the processing steps input data. To illustrate that much may be gained by optimal processing in SAR remote sensing, this section describes the steps involved in processing and touches upon many of the relevant research issues in the area.

The generation of SAR images from raw data, usually called SAR processing, is particularly difficult for airborne systems due to the effect of unpredictable motions of the airborne platform. These motions are generally measured using a global positioning system (GPS) in conjunction with an inertial measurement unit (IMU). During SAR processing, the measured motion must be taken into account. Generally, the degree to which this is necessary depends on the radar wavelength: the shorter the wavelength, the more disruptive an oscillating flight path is. Also, the extent to which motion compensation is possible, and the quality of the results obtained, depends on the SAR processing method used. In short, fast processing methods like wave number domain processing do not allow for accurate motion compensation without approximations, whereas prohibitively time consuming time-domain processing would allow motion compensation without approximations. Modern SAR processing techniques aim to achieve the optimal compromise between these extremes.

SAR interferometry is concerned with the derivation of topography and 3D object geometry from the phase differences between two sets of SAR data acquired from parallel flight passes separated by a short baseline. Among other things, the accuracy of interferometric processing depends on the knowledge of baseline geometry, i.e. the position of one antenna with respect to the other for each homologous data point whose interferometric phase difference is to be computed. Considering that the wavelengths of SAR sensors typically lie between a centimeter and a meter, and that the accuracy of interferometric phase difference measurements is required to lie in the range of a few degrees, baseline geometry should be known with an accuracy of less than a millimeter to a few centimeters at most. This cannot be achieved by GPS/IMU measurements. In case of spaceborne systems this deficit can easily be compensated by the use of one or more control points. In the case of airborne platforms, unpredictable motion makes this strategy infeasible. Therefore, approaches to

airborne repeat-pass interferometry estimate high-frequency motion parameters and correct baseline geometry based on the interferometric phase signal itself. Only then is the accuracy required for many applications achievable.

Range resolution of interferometric SAR imagery can be improved by combining the bandwidths of the interferometric partner data sets which are overlapping but not completely identical. This processing step can increase the potential for object extraction substantially.

The interferometric processing chain leads from two complex SAR image data sets to, for example, digital terrain models via processing steps such as coarse and fine image registration, common band filtering, coherence computation from the complex signals of corresponding pixel ensembles in the two data sets, semantic analysis of the resulting two by two coherence matrix, interferometric phase difference computation, phase unwrapping, and phase to height conversion. In the 1990's phase unwrapping has been a major challenge in research. Presently, it can be considered solved. The most robust solutions are resulting from multi-baseline configurations with different interferometric phase periodicity (i.e. fringe widths) for the different baselines.

In mapping applications, SAR polarimetry is concerned with the analysis of backscatter from the imaged objects as a function of polarisation. Fully polarimetric SAR data yield a two by two complex scattering matrix for each resolution cell, the elements of which are usually arranged in vector form. This vector, in the lexicographic basis, contains the signal corresponding to vertical, horizontal, and cross polarized transmission and reception. Before, for instance, classifying SAR pixels, the data is often transformed to another orthogonal basis which leads to a more direct and robust classification procedure due to an increased correspondence between components of the orthogonal basis and specific object characteristics and structure. Another quantity derived from scattering vectors of an ensemble of neighboring pixels is the three by three covariance matrix (or, alternatively, the coherence matrix). The investigation of its eigenvalue decomposition and its application to classification problems have been a major research topic in the past decade.

When interferometric SAR data is acquired in a fully polarimetric mode, a six by six coherence matrix can be computed from corresponding ensembles of neighboring pixels, and contains interferometric as well as polarimetric information. The analysis of this coherence matrix, i.e. polarimetric SAR interferometry, leads to 3D geometric information concerning the vertical structure of imaged objects.

When SAR data is not only acquired from two flight passes, as in interferometry, but from, for instance, a dozen flight passes displaced in the direction perpendicular to range and flight direction, it becomes possible to perform not only multi-baseline interferometric processing, but also a tomographic analysis of the imaged object space volume. This is particularly meaningful when the radiation is penetrating an object and all its components contribute to the backscatter, i.e. when volume scattering occurs.

From the various forms of SAR data, i.e. standard, interferometric, polarimetric, polarimetric interferometric, and tomographic configurations, semantic information is to be extracted. To apply the object extraction paradigm, consisting of structure and feature extraction, grouping and knowledge-based decision making, to the various types of SAR data in a theoretically well-founded and optimal fashion, the functional relations between objects and data, including the relevant stochastic properties, have to be explored and taken into account. Due to the large variety of SAR data available for object extraction, all approaches to the automated interpretation of data, such as data mining, and the approaches to object categorization explored by the computer vision academic community, are expected to prove extremely valuable in the extraction of semantic information from SAR data. As some SAR techniques have only recently been developed, the sensor specifics of object extraction can be expected to be a fruitful area of research in coming years.

In the following, we will discuss some of the issues which have been touched upon in this section: interferometric baseline correction, range resolution improvement from interferometric pairs, tomography compared with polarimetric interferometry, salient region feature extraction from

polarimetric SAR data, self-initializing classification of polarimetric interferometric data, and building extraction from polarimetric interferometric data. They present a selection from the research topics that have been investigated at the TU Berlin Computer Vision and Remote Sensing group in the last three to four years. By no means do they cover the full spectrum of research issues outlined in this section. Nevertheless, they present some particularly relevant aspects and serve to illustrate the current challenges in SAR remote sensing research. In order to make the material in the following sections informative to non-experts, general introductions to each topic, including references to the relevant literature, are given, and the results of the investigations are summarized. For an in depth explanation of the Berlin group's work we refer to other publications. Finally, we summarize results of the EuroSDR sensor and data fusion contest on techniques for mapping from airborne SAR and optical imagery, and outline future expectations.

2. BASELINE CORRECTION IN AIRBORNE REPEAT-PASS INTERFEROMETRY

Airborne SAR systems usually record the platform movement to later carry out motion compensation during data processing. However, any motion compensation approach is restricted by the quality of the sensor's navigation system, which is nowadays typically limited to a precision of about 1 to 5 cm. Uncompensated motion errors are causing artifacts in the images, among the most important are geometric distortions and phase errors. If a high-precision navigation system is used, such errors are often very small and can be neglected in most applications.

However, this is not the case for interferometric repeat-pass systems. Residual motion errors of each



Figure 1: Scene coherence

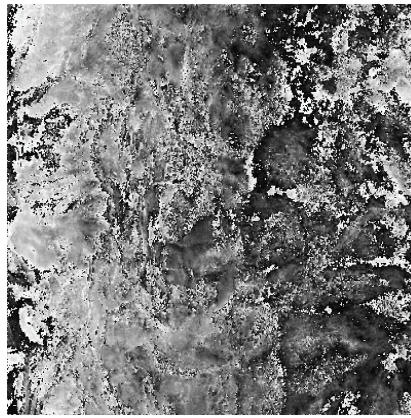


Figure 2: Initial interferometric phase after subtraction of topographic phase



Figure 3: Phase correction due to estimated baseline variations

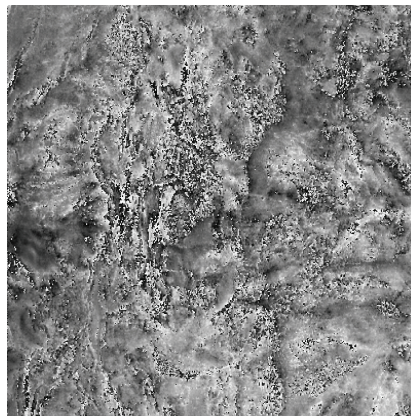


Figure 4: Final interferometric phase after subtraction of topographic phase

flight track are independent and do not cancel out during interferogram generation. Differently from single-pass systems, residual motion errors introduce an unknown time-varying baseline error. Even in case of a high-precision navigation system, this effect may cause significant phase errors in range and azimuth direction, in principle corresponding to the projection of the time-varying baseline error onto the radar line-of-sight.

There have been some efforts to estimate time varying baseline errors from the processed interferometric SAR (InSAR) data itself and to correct them in a post-processing step (Reigber, 2001; Prats & Mallorqui, 2003; Prats et al., 2003). However, all of these methods have certain limitations. They either fully account for the range-dependency of residual phase errors but are

unstable in case of low coherence, or they provide only a one-dimensional solution but are very stable in case of decorrelated data sets. Recently, (Reigber et al., 2005) have proposed a refined method for the estimation of time-varying baseline errors which uses the same principles as the two prior methods, but combines the advantages of both. Several sub-aperture interferograms are formed whose comparison is used to infer baseline errors. A two dimensional solution is calculated by a least-squares based estimation of time varying baseline errors, allowing to correctly take into account the variation of phase errors along azimuth and range direction. In a subsequent step, an external digital elevation model is incorporated for the detection of linear components of the baseline error along azimuth as well as constant baseline offsets.

Figure 1 shows coherence of a test data set. Processing this data is difficult in low coherence areas which can be seen in Figure 2 showing interferometric phase reduced by strongly smoothed topographic phase, thereby visualizing all disturbing effects. The systematic, mainly azimuth dependent behavior of the correction phase (Figure 3) demonstrates the plausibility of the results. Figure 4, as counterpart of Figure 2, contains interferometric phase reduced by topographic phase after baseline correction. The disturbing effects have largely vanished.

3. RANGE RESOLUTION IMPROVEMENT FROM INTERFEROMETRIC PAIRS

Resolution enhancement can be achieved by combining two images acquired in an interferometric imaging mode. It is based on the observation that the spectra of two SAR images, obtained from slightly different look angles, contain different parts of the ground reflectivity spectrum. This effect is known as the “wave number shift” in SAR interferometry (Gatelli et al., 1993). Figure 5 illustrates that due to the slight change in the look angle, different parts of the ground object spectrum are measured by the sensor. The basic principle of range resolution improvement is to coherently combine the different parts of the measured spectra, in order to increase the total range bandwidth. The spectra in both images partially overlap, and can be combined to obtain the new spectrum, if continuity is ensured. In this way, an image with enhanced range resolution can be computed.

Up to now, this idea was applied only to spaceborne data (Gatelli et al., 1993; Prati & Roca, 1993; Suess et al., 1998). In cases where the topography does not include steep gradients, a constant wave number shift can be assumed for the whole scene. In the airborne case, this is not so. Here, the wave number shift between two interferometric images varies strongly over the scene due to variations in incidence angle. However, with airborne sensors it is a relatively simple task to acquire, in addition to a single data set, a second data set by using an interferometric imaging geometry with a larger baseline. This makes the method of range resolution improvement highly attractive for airborne sensors.

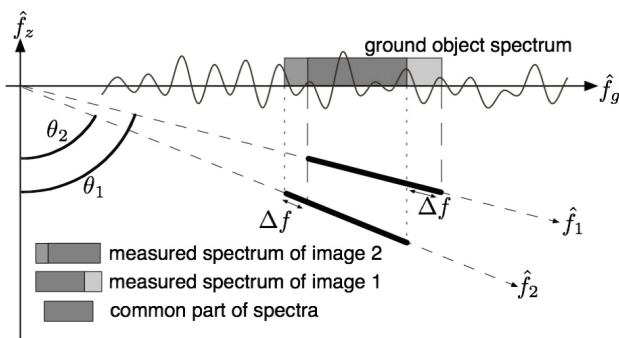


Figure 5: The spectral shift principle in frequency domain

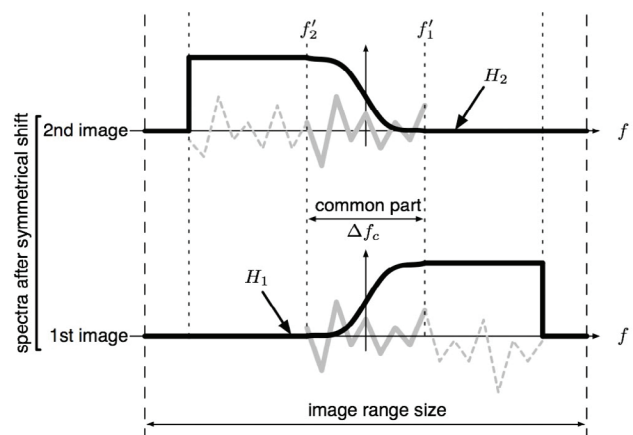


Figure 6: Smoothed spectral combination using a weighting filter.

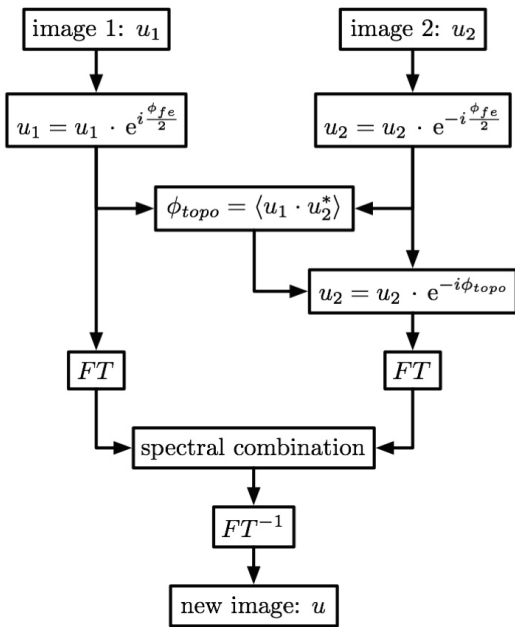


Figure 7: Block diagram of the proposed range resolution improvement algorithm. FT denotes a line-wise Fourier transform in range.



Figure 8: Original resolution

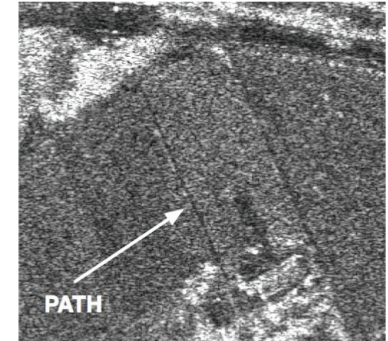


Figure 9: Improved resolution.

In the first part of the algorithm proposed by (Guillaso et al., 2005a) the influence of topography on the spectral shift is ignored. As the curvature of the flat earth phase corresponds exactly to the range dependence of the spectral shift, a symmetric phase correction can be applied to both images being equivalent to the flat earth correction. In a second step a smoothed, i.e. noise-reduced, version of the topographic phase is removed, in cases with moderate topography from the second image, in cases of more pronounced topography symmetrically from both images. Then the images spectra are combined in frequency space using a weighting filter over the common part of the spectra in order to avoid discontinuities in the final spectrum. The shape of the weighting function can for instance be one half of a Hanning function (c.f. Figure 6). Figure 7 summarizes the algorithm. Figures 8 and 9 show images with the original and the improved resolution, respectively.

4. TOMOGRAPHY AS A MEANS TO VALIDATE POLARIMETRIC INTERFEROMETRY

SAR tomography is concerned with focusing several SAR images in the third dimension perpendicular to range and azimuth directions, in order to image volumetric objects such as forests or cities.

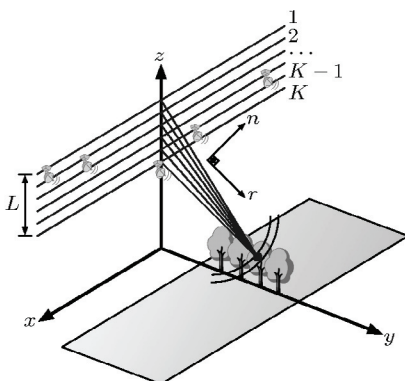


Figure 10: Geometry of a tomographic imaging configuration

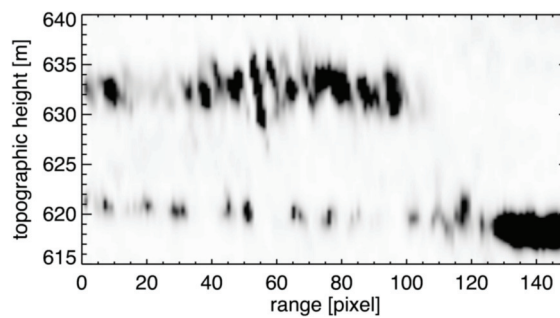


Figure 11: Vertical slice through tomographic data of a forest

This means that a synthetic aperture is formed along the direction perpendicular to the radar line of sight and the flight line using an imaging geometry similar to the one illustrated in Figure 10. The geometry of tomographic data

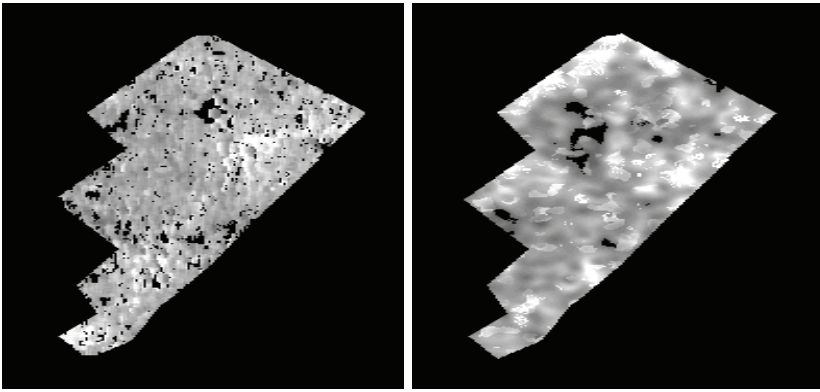


Figure 12: Forest height estimated by tomography

Figure 13: Forest height estimated by polarimetric interferometry

acquisition typically consists of several interferometric tracks non-uniformly spaced, which observe the same scene. From the resulting volumetric data set 3D profiles may be extracted allowing to detect targets under a covered volume or to generate 3D representations of the scene under study.

Commonly, tomographic SAR data are processed using a two step spectral analysis (SPECAN)

algorithm. The first step is a deramping of the signal, which corrects the quadratic phase variation occurring during tomographic data acquisition (Reigber & Moreira, 2000). After deramping, the spatial frequencies of the signals depend only on the height of the occurring scattering processes. The height of a scatterer can then be revealed by means of spectral estimation techniques such as Fourier, Capon, or MUSIC (Stoica & Moses, 1997).

(Reigber et al., 2005) estimate forest height and ground topography by means of polarimetric interferometry and tomography. In polarimetric interferometry, one of the most important methods described in the literature is the line-fitting approach in the complex unitary circle (Cloude & Papathanassiou, 2003). Although it has shown its principal potential, an open issue is the precise validation of the estimated parameters, as ground-truth collection is an extremely complex task in the case of forest parameters. SAR tomography is an alternative technique which generates a fully three-dimensional representation of the imaged scene through coherent combination of a greater number of tracks (Guillaso & Reigber, 2005). Forest ground and canopy are directly visible in a tomographic (volumetric) image. Figure 11 visualizes a vertical slice through a data set containing tree crowns and terrain surface underneath of the trees. Figures 12 and 13 show a good agreement between tree height estimates from tomography and polarimetric interferometry for effective baselines between 10 and 20 m using an L-band SAR data set.

5. SALIENT REGION EXTRACTION FROM POLARIMETRIC IMAGERY

Feature extractors, for instance edge detectors, act as concentrators of information that emphasize certain relevant properties of an image and suppress noise and other types of irrelevant information. This process is essential to algorithms which aim to provide high level, semantic interpretations of image content. A number of feature extraction operators have been proposed in the context of polarimetric SAR data. Ideally, these operators are designed to take the statistical properties of SAR images into account. Examples include polarimetric edge detectors (Schou et al., 2003) and texture descriptors (Grandi et al., 2004).

An important class of operators, point of interest and region of interest (ROI) detectors, has not yet been developed for SAR remote sensing data. ROI operators identify distinctive, prominent or highly informative patches in an image, and are employed to achieve sparse but succinct representations of complex image data. A wide range of problems in the automated analysis of image data can be formulated as search problems, where there is a need to identify certain objects or segments of a scene. In these types of problem, an operator which reduces an entire image to a comparatively small collection of patches, which are localized and have a known size, can greatly reduce the size of the search space to be considered.

In practice, ROI operators are designed to detect salient regions in an image, such as the corners of an object, distinctive object parts, or other localized regions of exceptional information density. Examples of such operators are given by (Kadir & Brady, 2001) and (Lowe, 2004). In contrast to interest point detectors, region detectors necessarily operate over a range of scales: as well as identifying distinctive image locations, they are also required to select an appropriate region size, or scale. The mechanism for scale selection is arguably the most important and difficult component of a ROI detector.

The applications for this type of operator are numerous and include, for example, the coregistration of stereo images in photogrammetry, and the identification of distinctive object parts in modern approaches to object categorization (Fei-Fei et al., 2003). Both of these applications are also of interest in SAR remote sensing. The task of data fusion could be simplified by the automated matching of ROIs, and new types of object models involving ROIs could enable improved performance in approaches to SAR scene understanding.

(Jäger & Hellwich, 2005) describe a ROI operator designed to identify distinctive regions in scale invariant fashion. It includes a novel definition of image entropy, in the information theoretical sense, for polarimetric SAR image content, as well as a rigorous statistical analysis of the operators scale selection mechanism. This analysis establishes the ability to identify a region irrespective of its size, which is e.g. measurable in number of pixels belonging to the region. We define the change in window content with scale (i.e. the content gradient) as a function of the changes of histograms

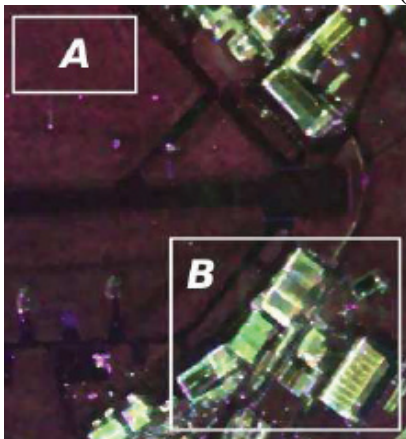


Figure 14: A fully polarimetric image of the DLR campus in Oberpfaffenhofen

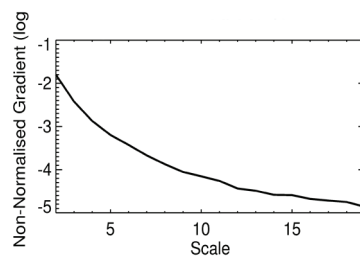


Figure 15: Biased content gradient as a function of scale

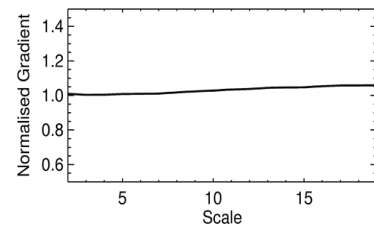


Figure 16: Unbiased content gradient as a function of scale

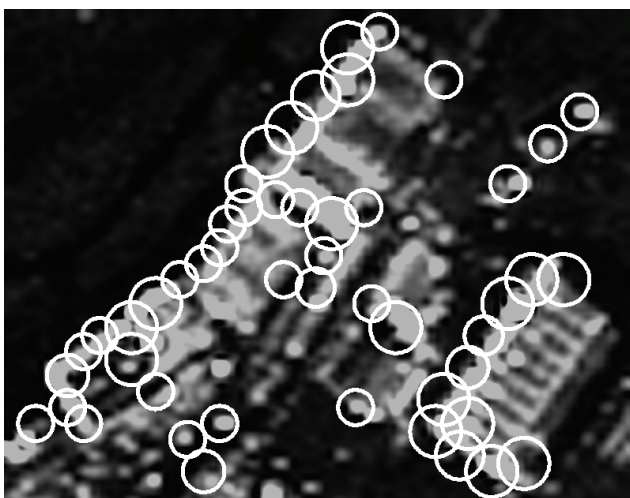


Figure 17: ROIs detected at original resolution

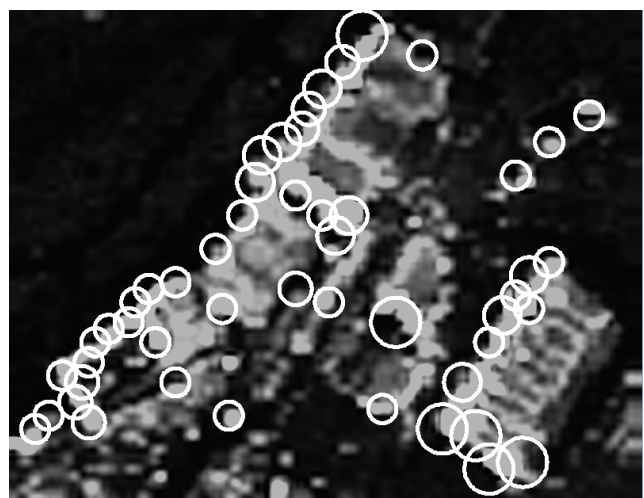


Figure 18: ROIs detected after reducing the original resolution by 30 %

belonging to neighboring scale space representations. When it is computed naively from the original pixels belonging to the regions, a scale or region size dependent bias occurs. This bias can be removed when rigorously accounting for statistical sample sizes.

The operator has been applied to real SAR data. Figure 14 shows the test areas A and B used to evaluate the operator. Area A is part of a homogeneous region, while area B contains buildings and other objects. Figures 15 and 16 illustrate the effect of eliminating the bias in the computed content gradient over area A. While Figure 15 shows the originally impressively large bias, Figure 16 demonstrates that it can virtually be completely removed. Figures 17 and 18 show the ROIs extracted from image data with varying resolution over area B. The data has been simulated by reducing the resolution of the input image of Figure 18 by 30 % with respect to the input for Figure 17. Scale invariance is achieved to a reasonable extend as the scales and locations of the salient regions – marked by circles of varying sizes – in the figures show.

6. CLASSIFICATION OF POLARIMETRIC INTERFEROMETRIC DATA

Unsupervised classification is often essential in the automated analysis of SAR remote sensing data. Classification results make data easier to interpret by users, and can serve as a starting point for automated analysis techniques that apply to homogeneous regions of a particular type of land cover. The classification of polarimetric interferometric (PolInSAR) data, in particular, is important, as this type of data has been shown to contain a wealth of information that is not obtainable by polarimetry or interferometry alone. Of special interest is the fact that PolInSAR data contains

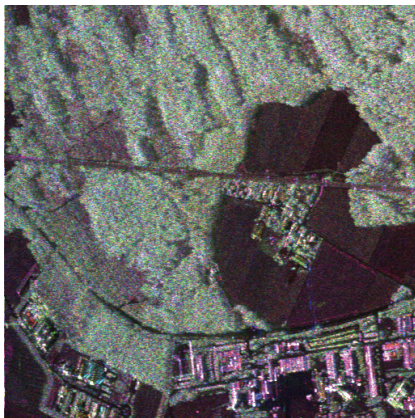


Figure 19: PolInSAR test data set

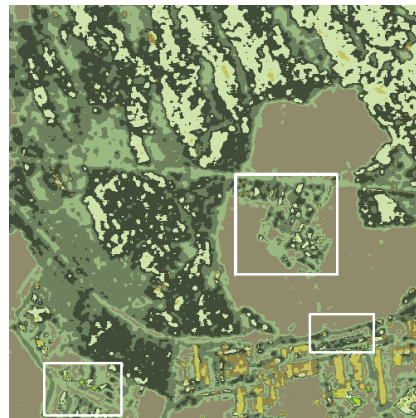


Figure 20: Classification using only polarimetry

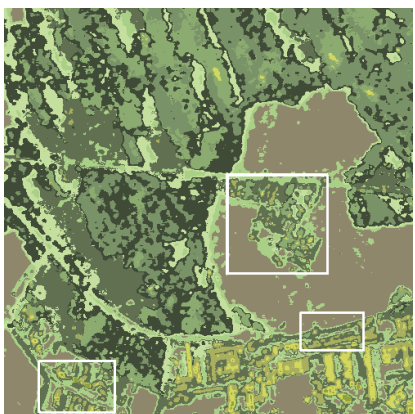


Figure 21: Classification using polarimetry and interferometry



Figure 22: Classification of interferometric phase differentials

information concerning the vertical structure of the scene under observation. This type of information is potentially useful in the analysis of forest, agricultural and urban areas.

A number of PolInSAR classifiers have been proposed in the past, including classifiers that are able to distinguish different types of forest with a high degree of accuracy (Lee et al., 2005; Ferro-Famil et al., 2005). These classifiers have demonstrated that interferometric information, in the form of (optimized) coherences, is essential in the segmentation of data containing volumetric structures. Interferometric information also makes the discrimination of man-made structures possible in cases where polarimetric information alone is ambiguous (Guillaso et al., 2005). Most of the methods proposed to date have, however, some shortcomings.

The six by six covariance matrix is commonly employed in the iterative determination of class parameters. This process faces three problems: (1) As these matrices contain the absolute phase of the complex coherence, the classification is sensitive to topography, which is undesirable in the identification of land cover types. (2) In addition, the degree of coherence, which is implicit in these matrices, is a biased estimator of the true coherence (Touzi & Lopes, 1996). This effect leads to lower contrast and, as a consequence, lower classification sensitivity over regions with low coherence. (3) Finally, these classifiers usually rely on arbitrary thresholds for initialization. Although these initializations perform well in practice, it is conceivable that some datasets have a structure that is not well represented by the particular choice of thresholds. Classes that extend to both sides of a threshold can be misrepresented in the classification result.

A classifier proposed by (Jäger et al., 2005) aims to address some of these difficulties. It takes into account the distributions of polarimetric class content, in the form of a Wishart distribution over coherence matrices, the absolute degree of interferometric coherence in several polarizations, and the change in interferometric phase as a function of polarization (interferometric phase differentials). By treating the degree of coherence separately, it is possible to make unbiased estimates of the true degree of coherence in a class, and the information inherent in interferometric phase differentials is both independent of topography and contains information regarding the vertical structure of the scene under observation.

Figure 19 shows a PolInSAR data set used to evaluate the classifier. Figure 20 shows the classification obtained for ten classes using only polarimetric information; Figure 21 shows the corresponding result using polarimetric and interferometric information. The buildings in the center and the lower left boxes of Figure 21 are identified correctly, where polarimetric information alone appears to have been insufficient and incorrect classifications as forest have occurred. Figure 22 illustrates the information content inherent in the interferometric phase differentials. The classification result with two classes was obtained using only the distribution over interferometric phase differentials. The classes clearly differentiate regions with a vertical structure, such as forest and buildings, from flat surfaces.

7. BUILDING EXTRACTION FROM POLARIMETRIC INTERFEROMETRIC DATA

One of the main applications in urban remote sensing is the analysis of buildings. This process consists of, firstly, the differentiation of buildings and surroundings, and, secondly, the characterization of located buildings. Building characterization generally consists of retrieving all relevant parameters concerning a building: shape (length, width) and height. In the scope of our studies, it is reduced to the estimation of their height.

We proposed a polarimetric interferometric method to localize and characterize buildings, using L-band SAR data, by linking the physical nature of a scatterer with its spatial geometry (Guillaso et al., 2003; Guillaso et al., 2004). This approach consists of three stages. The building localization is performed using polarimetric and polarimetric interferometric segmentation. The polarimetric segmentation is based on an unsupervised Wishart $H/A/\alpha$ (entropy, anisotropy, α -angle) classification scheme. An interpretation is attached to the resulting clusters using parameters obtained from the eigendecomposition of a sample coherence matrix, and the observed scene is classified to identify three general types of scattering mechanisms: single bounce, double bounce, and volume. Due to the overlap of the volume and double bounce classes, an additional classification based on a polarimetric/interferometric technique is applied to the volume class. For these areas optimal coherences, introduced in (Cloude & Papathanassiou, 1998), are used as new input to an unsupervised Wishart classification. In order to compensate for misclassifications in the building class, an analysis of the interferometric phase, given by the high resolution ESPRIT (Estimation of Signal Parameters via Rotational Invariance Techniques) method, is used. Using these interferometric

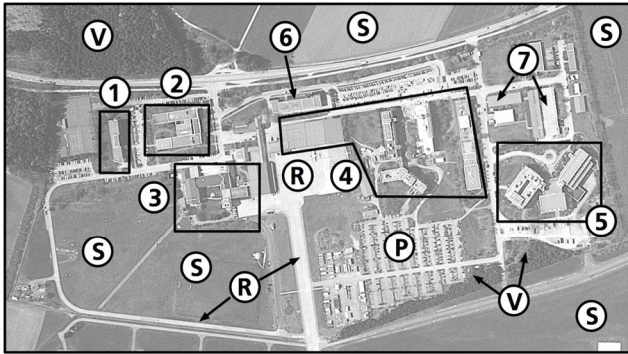


Figure 23: Aerial photograph of the DLR test site

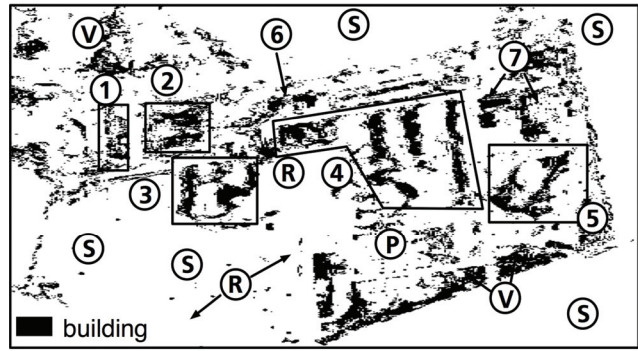


Figure 24: Initial mask of building locations

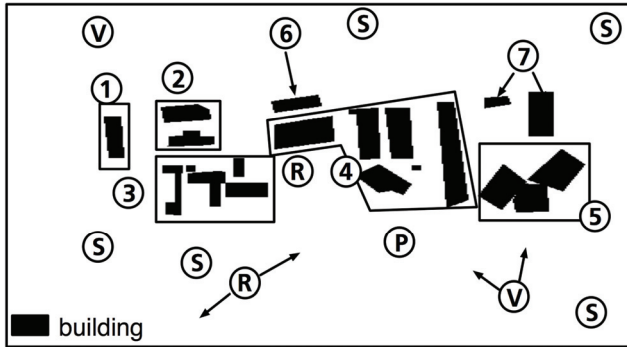


Figure 25: Final building locations

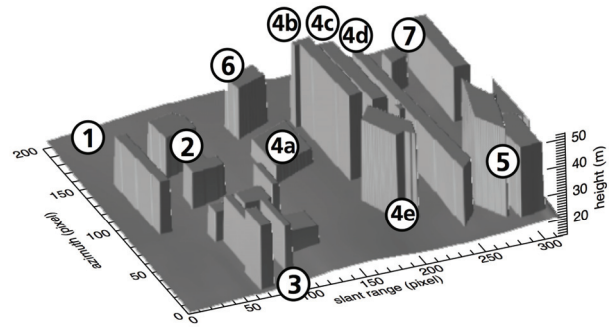


Figure 26: 3-D representation of buildings

phases, a phase-to-height conversion procedure is applied over building locations to retrieve building heights.

The proposed method was validated using polarimetric interferometric SAR data acquired over the Oberpfaffenhofen test site. These data were acquired in L-band (0.23 m wavelength) repeat-pass mode by the DLR E-SAR system. The spatial resolution of the data used is 1.5 m in range and azimuth. The interferometric baseline used is about 6.0 m. The area under study was the DLR site, which has some isolated buildings surrounded by complex media like green fields, roads, and forests. Figure 23 shows an aerial photograph of the chosen test site. Numbers (1) to (7) indicate the locations of the buildings under study. The other media present in the scene are roads (R), forests (V), fields (S), and a parking lot (P). Figure 24 shows an initial mask of building locations obtained after applying a polarimetric interferometric segmentation corresponding to the double bounce class. Some vegetation areas (V) are also classified as building. Figure 25 shows a mask of building locations obtained manually from Figure 24 after an analysis of interferometric phase given by the ESPRIT algorithm. Figure 26 is a 3-D representation of building groups (1) to (7). It is obtained by calculating the average height from phase in each building in the mask of Figure 25. The standard deviation of height estimation was found to be approximately ± 3 m.

8. THE POTENTIAL OF AIRBORNE SAR FOR MAPPING APPLICATIONS

Presently, the computer vision and remote sensing group at TU Berlin organizes a sensor and data fusion contest titled "Information for mapping from airborne SAR and optical imagery" under the auspices of the European Association for Spatial Data Research (EuroSDR). The contest aims to assess the relative merits of airborne SAR data and optical imagery in the task of topographic mapping. The issues under investigation include the question of whether SAR can compete with optical sensors for topographic mapping, and what could be gained by using SAR and optical data

in combination. The SAR data used in the test has spatial resolutions between 1.5 and 4 m. Three out of the four data sets are fully polarimetric.

To summarise the preliminary answers to the contest's questions after completion of the first stage, visual interpretation, it appears that SAR performs as well as optical sensing for extended areas and line objects, but is not as satisfactory with respect to smaller objects (Bellmann & Hellwich, 2005). This might change when using modern airborne SAR data with resolutions in the range of decimeters, where full speckle filtering can be applied without adversely affecting data interpretability as a consequence of the associated reduction in resolution. Furthermore, the test demonstrates that, without training the human interpreters in the identification of railways and other unfamiliar objects, it is nearly impossible to correctly classify SAR images. Due to the similarities between the human visual system and optical imaging, interpreting optical imagery is much easier.

In this paper we have summarized some of the research in the field of SAR remote sensing. The aims of the work are (1) to provide the SAR data to users in optimal quality, (2) to develop methods for classification and object extraction of interest to the mapping community, and last but not least (3) to explore the extraction of information that is specific to the SAR sensor, thereby helping to develop SAR remote sensing to its full potential, thereby support the application of SAR in mapping.

Considering the fast development of SAR sensing in the last two decades, we expect that SAR will further expand its share among sensors used in remote sensing. We try to support progress in research and development of airborne SAR systems by developing and maintaining the RAT (Radar Tools), open-source software package that provides implementations of numerous modern SAR processing and analysis algorithms (Reigber & Hellwich, 2004; Neumann et al., 2005).

9. ACKNOWLEDGEMENTS

We thank DFG (projects TOMOSAR and AGRIPOL) and DAAD (projects Acciones and Procope) for funding support of our work.

10. REFERENCES

- Bellmann, A., Hellwich, O. (2005): Sensor and Data Fusion Contest; Comparison of Visual Analysis between SAR- and Optical Sensors, Proceedings of 25. Wissenschaftlich-Technische Jahrestagung der DGPF '05, Rostock, Germany.
- Cloude, S.R., Papathanassiou, K.P. (1998): Polarimetric SAR Interferometry, IEEE Transactions on Geoscience and Remote Sensing, Vol. 36, No. 5, pp. 1551-1565.
- Cloude, S.R., Papathanassiou, K.P. (2003): A Three-Stage Inversion Process for Polarimetric SAR Interferometry, IEE Proceedings – Radar, Sonar and Navigation, Vol. 150, No. 3, pp. 125-134.
- De Grandi, G., Hoekman, D., Lee, J., Schuler, D., Ainsworth, T. (2004): A wavelet multiresolution technique for polarimetric texture analysis and segmentation in SAR images, Proceedings of IGARSS '04.
- Fei-Fei, L., Fergus, R., Perona, P. (2003): A Bayesian Approach to Unsupervised One-Shot Learning of Object Categories, Proceedings of ICCV '03, pp. 1134-1141.
- Ferro-Famil, L., Pottier, E., Lundsom, P., Moshammer, R., Papathanassiou, K. (2005): Forest Mapping and Classification Using L-Band PolInSAR Data, Proceedings of POLINSAR '05, Frascati, Italy.
- Gatelli, F., Guarneri, A.M., Parizzi, F., Pasquali, P., Prati, C., Rocca, F. (1993): The Wavenumber Shift in SAR Interferometry, IEEE Transactions on Geoscience and Remote Sensing, Vol. 29, No. 6, pp. 855-864.

- Guillaso, S., Ferro-Famil, L., Reigber, A., Pottier, E. (2003): Polarimetric Interferometric SAR Data Analysis Based on ESPRIT / MUSIC Methods, Proceedings of POLINSAR '03, Frascati, Italy.
- Guillaso, S., Reigber, A. (2005): Polarimetric SAR Tomography (POLTOM-SAR), Proceedings of PONLINSAR '05, Frascati, Italy.
- Guillaso, S., Ferro-Famil, L., Reigber, A., Pottier, E. (2005): Building Characterisation Using L-Band Polarimetric Interferometric SAR Data, IEEE Geoscience and Remote Sensing Letters, (in print).
- Guillaso, S., Reigber, A., Ferro-Famil, L., Pottier, E. (2005a): Range Resolution Improvement of Airborne SAR Images, IEEE Geoscience and Remote Sensing Letters, (submitted).
- Jäger, M., Hellwich, O. (2005): Saliency and Salient Region Detection in SAR Polarimetry, Proceedings of IGARSS '05, (in print).
- Jäger, M., Neumann, M., Guillaso, S., Reigber, A. (2005): The Distribution of Interferometric Phase Differentials and a Self-Initialising PolInSAR Classifier, Proceedings of EURAD '05, Paris, France.
- Kadir, T., Brady, M. (2001): Scale, Saliency and Image Description, International Journal of Computer Vision, Vol. 45(2), pp. 83-105.
- Lee, J., Ainsworth, T., Papathanassiou, K., Mette, T., Hajnsek, I. (2005): Forest Classification Based on L-Band Polarimetric and Interferometric SAR Data, Proceedings of POLINSAR '05, Frascati, Italy.
- Lowe, D. (2004): Distinctive Image Features from Scale-Invariant Keypoints, International Journal of Computer Vision, Vol. 60, pp. 91-110.
- Neumann, M., Reigber, A., Guillaso, S., Jaeger, M., Hellwich, O. (2005): PolInSAR Data Processing with RAT (Radar Tools), Proceedings of POLINSAR '05, Frascati, Italy.
- Prati, C., Roca, F. (1993): Improved Slant-Range Resolution With Multiple SAR Surveys, IEEE Transactions on Aerospace and Electronic Systems, Vol. 29, No. 4, pp. 135-143.
- Prats, P., Mallorqui, J.J. (2003): Estimation of Azimuth Phase Undulations with Multi-Squint Processing in Airborne Interferometric SAR Images, IEEE Transactions on Geoscience and Remote Sensing, Vol. 41, No. 6, pp. 1530-1533.
- Prats, P., Mallorqui, J.J., Reigber, A., Broquetas, A. (2003): Calibration of Airborne SAR Interferograms Using Multi-Squint Processed Image Pairs, Proceedings of SPIE' 03, Barcelona, Spain.
- Reigber, A., Moreira, A. (2000): First Demonstration of Airborne SAR Tomography using Multi-baseline L-Band Data, IEEE Transactions on Geoscience and Remote Sensing, Vol. 38, No. 5, pp. 2142-2152.
- Reigber, A. (2001): Correction of Residual Motion Errors in Airborne SAR Interferometry, IEE Electronic Letters, Vol. 37, No. 17, pp. 1083-1084.
- Reigber, A., Hellwich, O. (2004): RAT (Radar Tools): A free SAR Image Analysis Software Package, Proceedings of EUSAR'04, Ulm, pp. 997-1000.
- Reigber, A., Neumann, M., Guillaso, S., Sauer, S., Ferro-Famil, L. (2005): Evaluating PolInSAR Parameter Estimation Using Tomographic Imaging Results, Proceedings of EURAD '05.
- Reigber, A., Prats, P., Mallorqui, J.J. (2005): Refined Estimation of Time-Varying Baseline Errors in Airborne SAR Interferometry, IEEE Geoscience and Remote Sensing Letters, (submitted).
- Schou, J., Skriver, H., Nielsen, A. H., Conradsen, K. (2003): CFAR Edge Detector for Polarimetric SAR Images, IEEE Trans. on Geoscience and Remote Sensing, Vol. 41, No. 1, pp. 20-32.
- Stoica, P., Moses, R. (1997): Introduction to Spectral Analysis, N.J.: Prentice Hall.
- Suess, M., Völker, M., Wilson, J.J., Buck, C.H. (1998): Superresolution: Range Resolution Improvement by Coherent Combination of Repeat Pass SAR Images, Proceedings of EUSAR '98, Friedrichshafen, Germany.
- Touzi, R., Lopes, A. (1996): Statistics of the Stokes Parameters and of the Complex Coherence Parameters in One-Look and Multilook Speckle Fields, IEEE Transactions on Geoscience and Remote Sensing, Vol. 34, No. 2, pp. 519-531.